

TRANSFORMERLESS RESONANT CONVERTER BASED FOR AC MODULE APPLICATION

S.Dinesh kumar¹,S.Dinakarra²

P.G Student.¹, Asst professor², Department of Electrical Engineering
Sri Lakshmi Ammal Engineering College, Anna University, Chennai, India.
dineshkumarshanmugam88@gmail.com

Abstract: The proposed design features high efficiency over a wide input and output voltage range, step up voltage conversion, small size, and excellent transient performance. This aim of the project to improve the efficiency by using a scheme based on continuous conduction mode (CCM).Resonant DC-link inverter technique becomes dominate in solving the problems due to its simplicity in both power stage topology and control strategy. In addition, a resonant gate drive scheme is presented which provides rapid start up and low-loss at HF and VHF frequencies. The converter regulates the output using an on-off control scheme modulating at a fixed frequency. This control method enables fast transient response and efficient light load operation while providing controlled spectral characteristics of the input and output waveforms. The stability of the resonant converter in CCM has been verified at selected working conditions. The proposed single-stage inverter not only provides HPF to the utility line, but also achieves circuit simplicity, low cost, and high reliability.

I. INTRODUCTION

Motor drives rely on semiconductor power devices for power conditioning. The emergence of mature power devices, such as SCR, GTO and IGBT, makes it possible to handle power processing up to IMW. However the conventional PWM voltage source inverter (VSI) can not fully take the advantages of these advances in power semiconductor. Typically, VSI drive is suitable for dc/ac inverter applications in the power range of 10W-500kW[1]. This is mainly due to the following reasons:

- high switching losses at higher switching frequency;
- high dv/dt spikes;
- large SOA specifications required;
- high acoustic noise;
- poor ac line harmonics.

As has long been recognized, a substantial increase in inverter switching frequency is required

to be able to rumrmze low order harmonics in PWM-type applications. High switching frequencies have the concomitant advantages of higher current regulator bandwidth, smaller reactive component size, and for frequencies above 18kHz, acoustic noise which is above the threshold of human perception[2]. Basically, increasing switching frequency of motor drive has been accomplished following two approaches. By improving device speed and SOA ratings, from 500Hz to 2kHz, motor drives rated 1-25kW can be achieved[1]. The other approach to boost the switching frequency is based on improving the switching environment to maximize device utilization[I-5]. Using snubber circuit to reduce the switching losses and relieve high stresses is one of

most common methods. The principle of using snubber circuit to improve switching environment is modification of switching loci for a bipolar junction transistor (BJT). Unfortunately, the introduction of snubber circuit results in increased complexity of the drive circuit. Consequently, the increase in frequency is obtained with the heavy penalty 111 terms of high cost and low system efficiency.

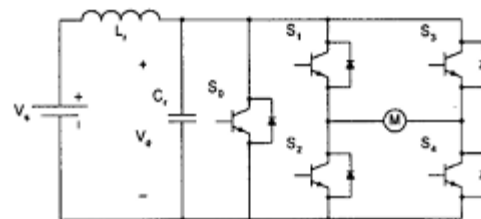


Fig. 1 Resonant DC-link inverter

Recent literature shows a new trend of incorporating resonant technique into conventional VSI topology. By introducing a resonant link

between the source and the switch network, zero-switching environment is created. Switching losses in these circuits are remarkably reduced. As a result, operation at high frequency up to 50kHz is possible to be achieved. In 1989, a resonant de-link inverter topology was proposed by D. M. Divan] 1], as shown in Fig. I. This circuit is attractive due to its simplicity in both power stage and control circuit. The principle of operation of the resonant de-link inverter will be described in the following section

II. PRINCIPLE OF OPERATION OF THE DC-LINK INVERTER

The operation of the resonant de link inverter can be found in [1,2,6,7]. A simplified circuit is illustrated in Fig. 2(a), in which I_0 represents the instantaneous current being supplied by the inverter to the motor.

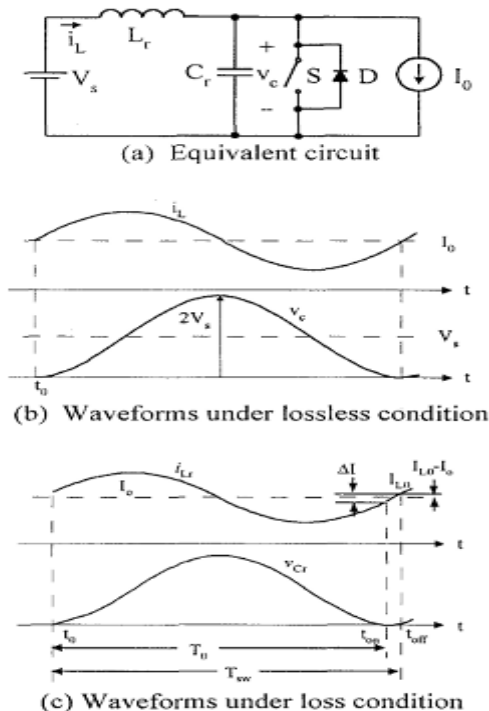


Fig. 2 Resonant dc-link inverter

(c) Waveforms under loss condition

Fig. 2 Resonant de-link inverter. Firstly, let's consider lossless case. Initially, the capacitor voltage $v_c(t_0)$ is zero and $i_{Lr}(t_0)$ is I_0 . It is easy to find that the capacitor voltage

$$v_{cr}(t) = V_s [1 - \cos(\omega(t-t_0))], \quad (1)$$

Where,

$\omega = 1 / \sqrt{L_r C_r}$. At $\omega(t-t_0) = \pi$, $v_{cr}(t)$ returns to zero and $i_{Lr}(t)$ returns to I_0 , thus setting up the desired switching condition for the switches in the inversion bridges. In this lossless case, S can be removed. Fig. 2(b) shows the resonant voltage and current waveforms of such an idealized circuit.

When conduction losses are considered, $i_{Lr}(t)$ and $v_{cr}(t)$ will no longer be able to return to I_0 and zero, respectively, at the end of each resonant cycle because of the damping effect. Thus the ZVS switching condition is lost. In order to compensate for the energy loss in each resonant cycle, a short interval is introduced by turning on and off S before the beginning of each resonant cycle so that the inductor current I_{L0} is greater than I_0 . The waveforms under such operation are shown in Fig. 2(c).

Assuming that the system is highly under-damped, $v_{cr}(t)$ can be expressed approximately as:

$$v_{cr}(t) = V_{dc} + e^{-R(t-t_0)/2L_r}$$

$$[\cos(\omega(t-t_0)) - \cos(\omega(t-t_0))] \quad (3)$$

It can be seen that the capacitor voltage depends on the difference between I_{L0} and I_0 . If the time period introduced is too long and I_{L0} is much larger than I_0 , then $v_{cr}(t)$ will have a peak value significantly larger than $2V_s$. Therefore, the interval during which S remains on must be controlled to ensure that $I_{L0} - I_0$ does not exceed the desired value. Because of this interval, the power switch is now driven on and off at a frequency Z , a little bit smaller than the resonant frequency of the L_r, C_r resonant tank.

Finally, it is interesting to note that in Fig. 2(a), switch S is in parallel with two switches comprising an inverter leg and hence it can also be removed, resulting in a more simplified inverter topology for the proposed ac drive application.

III. DESIGN OF 200HP MOTOR DRIVE

A. Control strategy

The primary objective of this work is to design a single phase high power (up to 200HP) motor drive. A load current command (with a certain phase advance) is given by a sinusoidal signal generator. Figure 3 shows one of the drive strategies for the resonant de-link inverter shown in Fig. 1. In this strategy, the load current $i_M(t)$ is compared with the current command $i_{cmd}(t)$. By sampling the compared result at the end of each switching cycle, the control circuit determines the conduction mode of the four switches in next switching cycle. The control rule is:

$$\text{Sign}[i_{cmd}(t_k)] \cdot \text{Sign}[|i_{cmd}(t_k)| - |i_M(t_k)|]$$

$$= \begin{cases} +1 & \text{--- } S_1, S_4 \text{ ON; } S_2, S_3 \text{ OFF} \\ -1 & \text{--- } S_2, S_3 \text{ ON; } S_1, S_4 \text{ OFF} \end{cases}$$

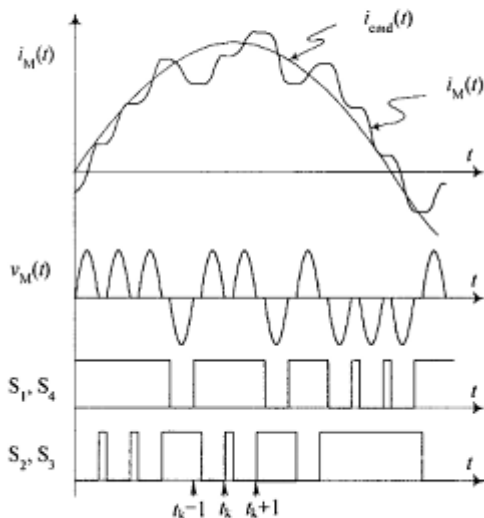


Fig. 3 Control strategy for resonant dc-link inverter

In the beginning of each switching cycle, let's have a short interval Δt , during which, all the four switches will be turned on so that the resonant tank can get energy compensation as mentioned in Section II.

B. Design procedure

Constraint 1: Set the linear increment of resonant inductor current ΔI for energy compensation in each switching cycle (shown in Fig. 2(c)) as

$$M = 1\% \times I_0 \quad (4)$$

Constraint 2: The peak resonant inductor current

$$I_{Lr, pk} = 6kA. \quad (5)$$

Constraint 3: The peak resonant capacitor voltage

$$V_{Cr, pk} = 1kV. \quad (6)$$

Constraint 4: Resonant inductance is much smaller than the load inductance:

$$L_r \ll L. \quad (7)$$

Based on the four constraints, a 200HP resonant de-link inverter is designed as follow.

Specifications:

Load (motor parameters):

$$L = 11.48 \text{ mH};$$

$$R = 0.624 \text{ m}\Omega;$$

$$V_{emf} = 134.3 \text{ V (rms)}$$

Switching frequency, $f_s = 50 \text{ kHz}$ ($T_{sw} = 20 \mu\text{s}$)

Output fundamental frequency, $f_o = 1.632 \text{ kHz}$

Output current: $I_0 = 1170.6 \text{ A (rms)}$

Phase advance: $\phi = 30^\circ$

Input voltage: $V_{dc} = 350 \text{ VDC}$

Design:

By neglecting the exponential attenuation in Eq.(3) we have

$$V_{Cr}(I) = V/\epsilon + [Z, (I L_0 \pm i_M(I)) \sin \theta V - V_{dc} \cos \theta V] \quad (8)$$

$$i''(t) = i_M(t) + [\sim: \sin \theta \omega' + (1, 0 \pm i_M(I)) \cos \theta \omega'] \quad (9)$$

Where

$$Z_0 = \text{root of } L_r / C_r \quad (10)$$

Basically, the task of design for a resonant circuit is to determine the value of resonant inductance L , and resonant capacitance C

In Eqs.(8) and (9), the "+" sign is applied

$$\begin{cases} I_{Lr,pk}^- \approx I_{o,pk} + \frac{V_{dc}}{Z_o} \\ I_{Lr,pk}^+ = I_{o,pk} + \sqrt{\left(\frac{V_{dc}}{Z_o}\right)^2 + (2.1 I_{o,pk})^2} \end{cases} \quad (12)$$
$$Z_o = \frac{V_{dk}}{\sqrt{(I_{r,pk}^+ - I_{v,pk})^2 - (2.1 I_{v,pk})^2}} \quad (13)$$

$$\frac{L_r}{L} = \frac{0.42 \mu H}{11.48 \mu H} \ll 1.$$

Voltage stress: 923V.

22

On the other hand, during the linear charging period of resonant inductor, we have

$$M = \frac{V_{dc}}{L} \cdot t = I \times 10\% = 117A \quad (14)$$

and,

$$t_{L,f} = T_w - t_s = 20\mu s - 2n \cdot LrCr \quad (15)$$

Solving Eq.(13)-(15) and considering

, we obtain the following design results:

$$L_r = 0.42mH; C_r = 24.0\mu F; t_{L,f} = 0.5\mu s.$$

Now, let's check Constran 3, $V_{cr,pk} < 1kV$, and Constran 4, $L_r < L$:

$$V_{Cr,pk} = V_{cr,pk} = V_{dc} + \sim (2.1 \times I_{o,pk} Z_0)^2 + r_s$$

$$= 350 + (2.1 \times 1650 \times \sim 0.42)^2 + 3502$$

resonant de-link inverter

Fig. 4 shows the schematic of the designed resonant de-link inverter together with its control circuit for the PSPICE simulation. The 200HP motor is modeled by a serial branch formed by L, R and back EMF V_{emf} . I_{com} is a sinusoidal current command, which has 30° phase difference leading the back EMF voltage. The load current is sensed by a transducer modeled by H with

a certain transform ratio. The output of H is compared with the current command to generate a signal for the D-flip-flop UIA and determine which of the switches S1 and S4 or Switches S2 and S3 must be turned on. The pulse voltage source v_p serves as synchronizing signal (with switching frequency) and its pulse width provides a short interval to turn on all the switches for energy compensation as mentioned in Section II.

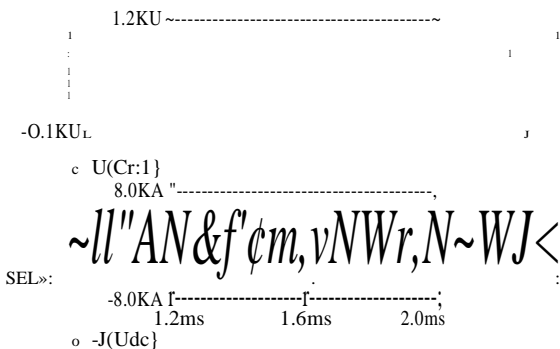


Fig. 5 Simulated capacitor voltage (upper) and input current (lower)

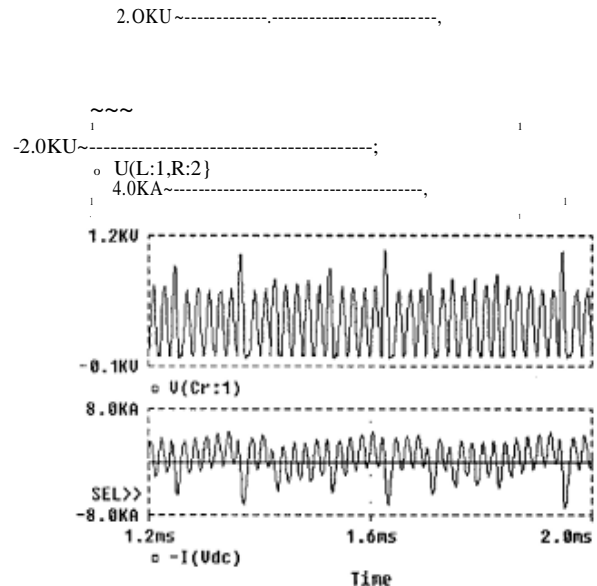


Fig. 6 Simulated motor voltage (upper) and current (lower)

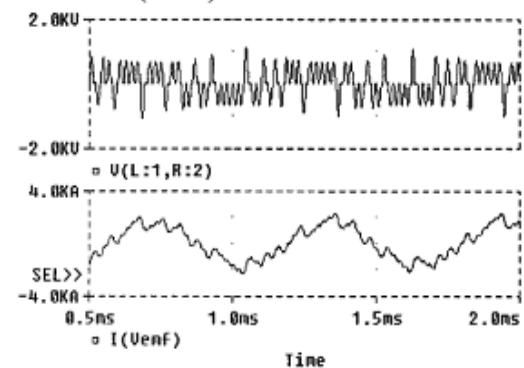


Fig. 7 Simulated motor voltage (upper) and current (lower)

Figure 7 shows the frequency spectra of the motor voltage and current waveforms. It can be seen that the harmonic components mainly exist in the low frequency range, implying less EMI.

VII. CONCLUSIONS

Resonant DC-link inverter is able to provide effective treatments for high EMI, acoustic noise, poor harmonic contents and low frequency operation problems. Both analysis and PSPICE simulation

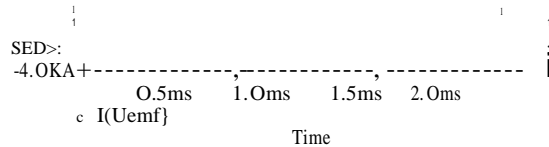


Fig. 6 Simulated motor voltage (upper) and current (lower)

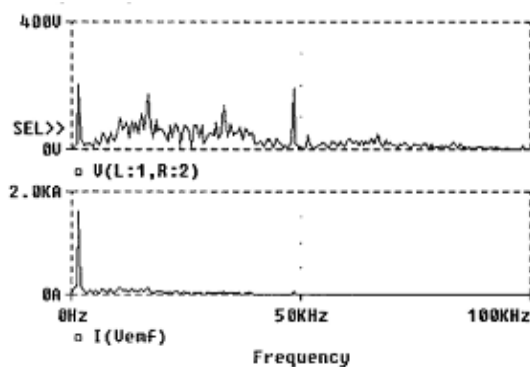


Fig. 7 Simulated frequency spectra of the motor voltage (upper) and current (lower)

The simulation results for the resonant de-link inverter are given in Figs. 5, 6 and 7. It is clearly shown in Fig. 5 that the motor voltage and the capacitor voltage are trains of resonant pulses that start and end at about zero volt. Thus it ensures the soft-switching for the switches. We also noticed that the maximum resonant capacitor voltage is about 1kV and the maximum supply current is about 7kA, which are close to the design specifications (V_{peak} : 1kV, I_{peak} : 6kA).

results show that at high frequency operation, the resonant DC-link inverter gives limited frequency range of harmonics, which ensures low EMI. The inverter efficiency is also significantly higher than its hard switching counterpart, implying the capability of high frequency operation. In the design of resonant DC-link inverter for high power applications, voltage and current stresses of switches are crucial. In selecting the switching devices, satisfying these stresses should be set as design constraints.

REFERENCE:

- [1]. B. Burger and D. Kranzer, "Extreme high efficiency PV-power converters," in Proc. 13th Eur.Conf. Power Electron. Appl. (EPE), 2009, pp. 1–13.
- [2]. C. Rodriguez and G. A. J. Amaratunga, "Long-lifetime power inverter for photovoltaic AC modules," IEEE Trans. Ind. Electron., vol. 55, no. 7, pp. 2593–2601, Jul. 2008.
- [3]. H. Patel and V. Agarwal, "A single-stage single-phase transformer-less doubly grounded grid-connected PV interface," IEEE Trans. Energy Convers., vol. 24, no. 1, pp. 93–101, Mar. 2009.
- [4]. R. H. Wills, F. E. Hall, S. J. Strong, and J. H. Wohlgemuth, "The AC photovoltaic module," in Proc. 25th IEEE Photovolt. Spec. Conf., 1996, pp. 1231–1234.
- [5]. S. B. Kjaer, J. K. Pedersen, and F. Blaabjerg, "A review of single-phase grid-connected inverters for photovoltaic modules," IEEE Trans. Ind. Appl., vol. 41, no. 5, pp. 1292–1306, Sep./Oct. 2005.
- [6]. T. Yu, J. S. Lai, H. Qian, and, "High-efficiency MOSFET inverter with H6-type configuration for photovoltaic non-isolated AC module applications," IEEE Trans. Power Electron., vol. 26, no. 4, pp. 1253– 1260, Apr. 2011.